



Effects of Tumour-induced Flow Patterns on Aerosol Drug Delivery

X. Guan^a, T.B. Martonen^b

^a*The Center for Extrapolation Modelling, Department of Medicine, Duke University, Durham, NC 27710, USA*

^b*National Health and Environmental Effects Research Laboratory, U.S. Environmental Protection Agency, Research Triangle Park, NC 27711, and Division of Pulmonary Diseases, Department of Medicine, University of North Carolina, Chapel Hill, NC 27599, USA, E-Mail: martonen@herl45.herl.epa.gov*

Abstract

This manuscript presents a theoretical study of fluid dynamics in diseased lungs. The objective was to describe fluid behavior and assist in the development of new techniques for targeted delivery of drugs. Numerical simulations were conducted using FIDAP on the Cray T90 supercomputer. Two lung bifurcations with tumors in tracheobronchial airways were considered. Weibel [1] lung morphology and Hofmann et al. [2] breathing parameters were employed. It has been observed that the effects of tumor size, rather than breathing conditions, dominate localized flow patterns around a tumor.

1 Introduction

Carcinomas attributable to air pollutants are too commonly observed among the global population [3-9]. Indeed, the *increasing* rate of lung cancers poses a great threat to the human health and well-being. To treat the disease, many medical techniques have been used; however, the problems persists. Therefore, new methodologies are needed.

In medical practice, tumors can be treated using aerosolized drugs. The particles are transported by inhaled air and deposited on airways walls. It is well known [10-13] that flow patterns can have pronounced effects on particle trajectories. Interactions between fluid dynamics and particle deposition in lungs have been well documented in the literature [14-19]. Traditional aerosol therapy protocol do not emphasize site-specific delivery. This naturally results



136 Simulations in Biomedicine IV

in the inefficient delivery of drugs to required sites (tumors), the overdose of drugs at non-diseased portions of airways, and the ineffectual use of drugs. An improved aerosol therapy technique would account for the site-specific pharmacokinetic action of medicinal agents.

To target the delivery of drugs onto diseased sites, localized flow patterns around tumors must be known. This work studied fluid motion within human lung bifurcations with tumors. The objective was to describe fluid behavior and, thereby, assist in the development of new techniques for targeted drug delivery. Numerical simulations were performed using FIDAP (computational fluid dynamics software) on the Cray T90 supercomputer. We performed a systematic investigation of the effects of tumor sizes and breathing conditions on fluid dynamics within the lung.

2 Methods

The numerical simulations of lung bifurcations with tumors involved three elements: fluid dynamics, airway morphology and ventilatory parameters. These factors are described in detail below.

2.1 Fluid motion

The computations were performed using FIDAP, which employs finite element methods to describe fluid motion. Flow in bifurcations is governed by the Navier-Stokes equation (momentum conservation)

$$\rho \left(\frac{\partial \mathbf{u}}{\partial t} + \mathbf{u} \cdot \nabla \mathbf{u} \right) = -\nabla p + \mu \nabla^2 \mathbf{u}, \quad (1)$$

and the mass conservation equation

$$\nabla \cdot \mathbf{u} = 0 \quad (2)$$

where ρ and μ are the density and absolute viscosity of air, \mathbf{u} is the velocity vector, t is time, and p is pressure. The mathematical symbols ∇ , $\nabla \cdot$, and ∇^2 are the gradient, divergence and Laplacian operators, respectively.

Steady state flows were considered in this work [20]. The governing equations (1) and (2) were solved with appropriate boundary conditions.

2.2 Lung morphology

Weibel [1] and Horsfield et al. [21] data were used to describe airway dimensions and spatial networks. The Model A of Weibel [1] is a symmetric, dichotomous branching system. There are 24 generations (I) of airways in the lung, where the trachea is denoted by $I = 0$. The whole lung is divided into tracheobronchial (TB) ($I = 0-16$, inclusive) and pulmonary (P) compartments ($I = 17-23$, inclusive).

In this work, we considered two bifurcations within the TB compartment, locations where carcinomas are most frequently observed [4-9]. The first

bifurcation is composed of upper bronchi ($I = 3-4$), and the second bifurcation is composed of intermediate airways ($I = 7-8$). The diameters (D) and lengths (L) of the airways are presented in Table 1. The bifurcation angles were 70° .

Table 1. Dimensions of airways within human lung bifurcations [1].

Dimension (cm)	Generation, I			
	3	4	7	8
Diameter	0.56	0.45	0.23	0.186
Length	0.76	1.27	0.76	0.64

In the cases addressed herein, tumors were simulated within bifurcations. The tumors were idealized as spheres with centers on the carinal ridges.

2.3 Breathing conditions

The ventilatory parameters which characterize breathing are the tidal volume (TV) and frequency (f). We simulated the five different activity levels prescribed by Hofmann et al. [2]. However, for brevity, only sedentary (TV = 500 ml, $f = 14$ breaths/min) and heavy (TV = 2449 ml, $f = 24.5$ breaths/min) breathing conditions will be presented. The corresponding average velocities (U) and Reynolds numbers ($Re = DU/\nu$, where $\nu = \mu/\rho$) for the two aforementioned bifurcations are listed in Table 2.

Table 2. Average velocities (U) and Reynolds numbers (Re) within parent tubes of bifurcations.

Bifurcation	Sedentary Breathing		Heavy Breathing	
	U, cm/sec	Re	U, cm/sec	Re
I = 3-4	118	442	1015	3791
I = 7-8	44	67	376	577

3 Results and discussion

We have conducted systematic simulations for a variety of tumor sizes and ventilatory parameters for bifurcations $I = 3-4$ and $I = 7-8$. To be succinct, we shall focus on two breathing conditions (resting and heavy activities) for tumor radius-to-daughter radius ratios, r/R , of 0.4 and 0.8. The ratio, r/R , reflects the relative size of the tumor to the cross-section of the daughter tube. A control case $r/R = 0$ represents a smooth-walled bifurcation (without a tumor). When $r/R = 2.0$, the cross-section of a daughter tube is blocked by a tumor. Since the illustrations below are self-explanatory, only a brief discussion will be necessary to orient the reader.

3.1 Upper airways (bifurcation 3-4)

3.1.1 Sedentary breathing

In Figure 1 the velocity vector fields are presented for a resting condition. The ratio r/R changes from 0.4 in Panel (a) to 0.8 in Panel (b). Clearly, the localized flow patterns near the carina are affected by the tumor. The fluid elements are



138 Simulations in Biomedicine IV

forced to change direction around the tumor. The velocities in the reduced cross-sectional area are accelerated to satisfy the principle of mass conservation. Data from our systematic simulations established that effects were initialized at a very small r/R ratio (i.e., 0.1). However, influences of a tumor were not pronounced until a critical value of $r/R = 0.8$. In particular, flow recirculation was not observed behind the tumor until $r/R \geq 0.8$.

3.1.2 Heavy breathing

When the physical activity increased, the flow patterns near a tumor changed, however, the flow rate did not influence flow patterns as significantly as tumor size. Figure 2 shows the velocity vector fields for exercise. Panels (a) and (b) are for $r/R = 0.4$ and 0.8 , respectively. For a fixed r/R ratio, although the magnitudes of the velocities are different (see Table 2), the flow patterns are similar (e.g., Figures 1(a) and 2(a)). Again, effects were first noted at $r/R = 0.1$ and the critical value of the r/R ratio was 0.8 .

3.2 Intermediate airways (bifurcation 7-8)

3.2.1 Sedentary breathing

These simulations were performed to study the effects of the tumor sizes and breathing conditions in other airway generations. Figure 3 illustrates the velocity vector fields for a resting condition. To be consistent with previous computations, the ratio r/R was 0.4 and 0.8 . As before, effects were observed at $r/R = 0.1$. The influences of the tumor are stronger at $r/R = 0.8$ than 0.4 . Effects were most pronounced when $r/R \geq 0.6$, this critical value is smaller than the 0.8 value for bifurcation 3-4.

3.2.2 Heavy breathing

Figure 4 shows the velocity vector fields for exercise. Similar to bifurcation 3-4, effects related to tumor size dominate localized flow patterns, not the magnitude of the flow rate. Again, effects were first noted at $r/R = 0.1$ and the critical value of r/R was 0.6 .

In conclusion, we have conducted systematic simulations of localized flow patterns in lung bifurcations with tumors. The computational results can be applied in medical practice to explore new techniques for targeted drug delivery. In aerosol therapy, drug particles are entrained by inhaled air and transported into the lung. Particles will be deposited onto airway walls by three major deposition mechanisms of inertial impaction, sedimentation and diffusion [15]. From our numerical data, several points can be made concerning the delivery of drugs to specific sites of disease.

(1) Large drug particles will be deposited on the anterior (front) surface of a tumor due to the mechanism of inertial impaction.

(2) For large tumors, small drug particles will be trapped in the recirculation zones. This increases the opportunities for deposition due to the processes of sedimentation and diffusion.



4 Summary

Flow patterns in human lung bifurcations were simulated to investigate the effects of tumor sizes and breathing conditions. The numerical simulations were performed using FIDAP on the Cray T90 supercomputer. The Weibel [1] lung morphology and Hofmann et al. [2] breathing parameters were employed to describe the airway dimensions and respiratory conditions. The localized flow patterns near tumors were observed to be significantly affected by tumor sizes. The critical values of the ratio of tumor radius-to-daughter radius, r/R , were 0.8 for bifurcation 3-4 and 0.6 for bifurcation 7-8. The breathing conditions did not produce as significant influences on localized flow patterns.

DISCLAIMER: This manuscript has been reviewed in accordance with the policy of the National Health and Environmental Effects Research Laboratory, U.S. Environmental Protection Agency, and approved for publication. Approval does not signify that the contents necessarily reflect the views and policies of the Agency, nor does mention of trade names or commercial products constitute endorsement or recommendation for use.

References

1. Weibel, E. R. Design of airways and blood vessels as branching trees, *The Lung: Scientific Foundations*, ed R. G. Crystal, J. B. West, P. J. Barnes, N. S. Cherniack & E. R. Weibel, Vol. 1, pp 711-720, Raven Press, New York, 1991.
2. Hofmann, W., Martonen, T. B. & Graham, R. C. Predicted deposition of nonhygroscopic aerosols in the human lung as a function of subject age, *J. Aerosol Med.*, 1989, 2, 49-68.
3. Hansen, H. H. (ed). *Lung Cancer. Advances in Basic and Clinical Research*, Kluwer Academic Publishers, Boston, 1995.
4. Shah, H., Garbe, L., Nussbaum, E., Dumon, J.-F., Chiodera, P. L. & Cavaliere, S. Benign tumors of the tracheobronchial tree. Endoscopic characteristics and role of laser resection, *Chest*, 1995, 107, 1744-1751.
5. Ferguson, M. K., MacMahon, H., Berkerman, C. & Ryan, J. W. Noninvasive and invasive staging of lung cancer, *Lung Cancer: A Comprehensive Treatise*, ed J. D. Bitran, H. M. Golomb, A. G. Little & R. R. Weichselbaum, pp 113-119, Grune and Stratton, Inc., Orlando, FL, 1988.
6. Chan, J. K. C., Hui, P. K., Tsang, W. Y. W., Law, C.-K., Ma, C.-C., Yip, T. T. C. & Poon, Y. F. Primary lymphoepithelioma-like carcinoma of the lung, *Cancer*, 1995, 76, 413-422.



140 Simulations in Biomedicine IV

7. Marcantonio, D. R. & Libshitz, H. I. Axillary lymph node metastases of bronchogenic carcinoma, *Cancer*, 1995, 76, 803-806.
8. Novotny, J. E. & Huiras, C. M. Resection and adjuvant chemotherapy of pulmonary blastoma, *Cancer*, 1995, 76, 1537-1539.
9. Roux, F. J., Lantuéjoul, S., Brambilla, E. & Brambilla, C. Mucinous cystadenoma of the lung, *Cancer*, 1995, 76, 1540-1544.
10. Martonen, T. B., Zhang, Z. & Lessmann, R. C. Fluid dynamics of the human larynx and upper tracheobronchial airways, *Aerosol Sci. Tech.*, 1993, 19, 133-156.
11. Martonen, T. B., Yang, Y. & Xue, Z. Q. Influences of cartilaginous rings on tracheobronchial fluid dynamics, *Inhal. Toxi.*, 1994, 6, 185-203.
12. Martonen, T. B., Yang, Y. & Xue, Z. Q. Effects of carinal ridge shapes on lung airstreams, *Aerosol Sci. Tech.*, 1994, 21, 119-136.
13. Martonen, T., Zhang, Z. & Yang, Y. Particle diffusion with entrance effects in a smooth-walled cylinder, *J. Aerosol Sci.*, 1996, 27, 139-150.
14. Martonen, T. & Yang, Y. Deposition mechanics of pharmaceutical particles in human airways, *Inhalation Aerosols. Physical and Biological Basis for Therapy*, ed A. J. Hickey, pp 3-27, Marcel Dekker, Inc. New York, 1996.
15. Martonen, T. B. Mathematical model for the selective deposition of inhaled pharmaceuticals, *J. Phar. Sci.*, 1993, 82, 1191-1199.
16. Martonen, T. B. & Katz, I. Deposition patterns of polydisperse aerosols within human lungs, *J. Aerosol Med.*, 1993, 6, 251-274.
17. Martonen, T. B. & Katz, I. M. Deposition patterns of aerosolized drugs within human lungs: effects of ventilatory parameters, *Phar. Res.*, 1993, 10, 871-878.
18. Martonen, T. B. & Katz, I. M. Inter-related effects of morphology and ventilation on drug deposition patterns, *S.T.P. Phar. Sci.*, 1994, 4, 11-18.
19. Martonen, T., Katz, I. & Cress, W. Aerosol deposition as a function of airway disease: cystic fibrosis, *Phar. Res.*, 1995, 12, 96-102.
20. Yang, Y. & Martonen, T. B. Flow dynamics in human respiratory and circulatory systems, *Inhal. Toxi.*, 1996, 8, 877-901.
21. Horsfield, K., Dart, G., Olson, D. E., Filley, G. F. & Cumming, G. Models of the human bronchial tree, *J. Appl. Physiol.*, 1971, 31, 207.

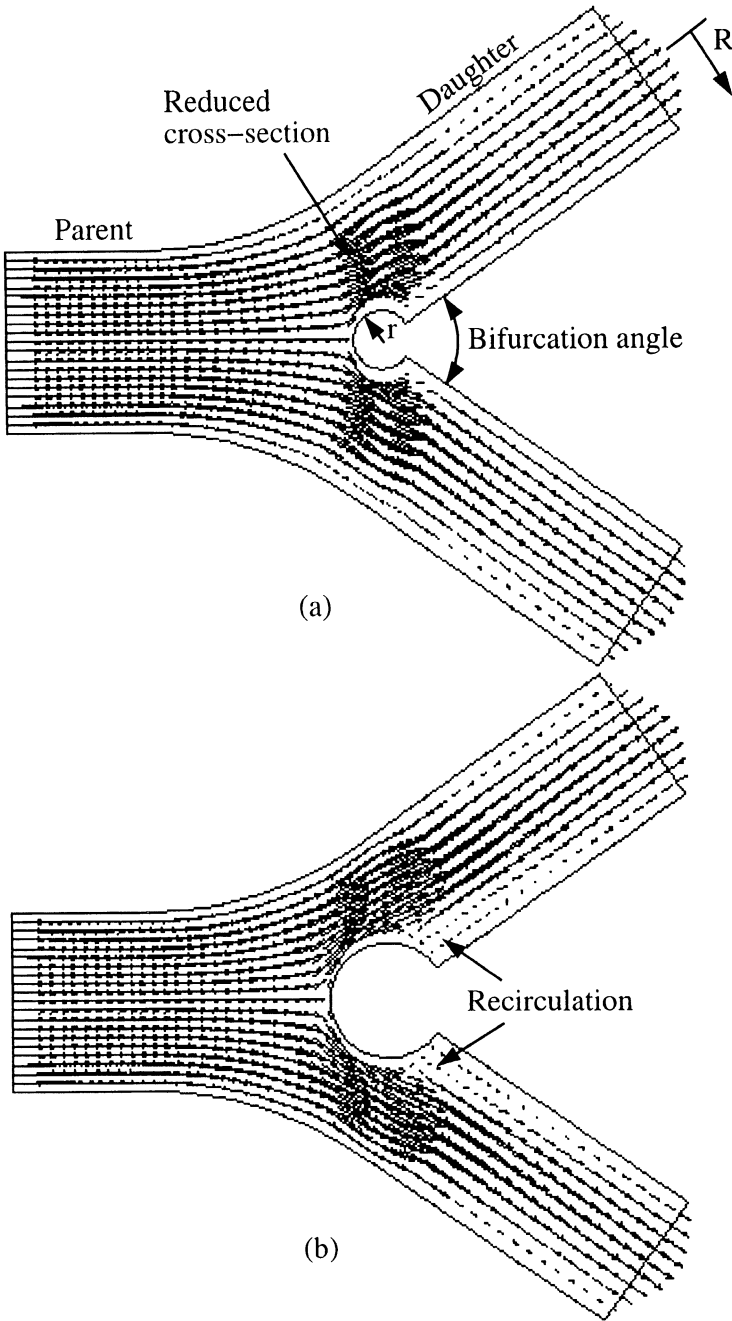


Figure 1: Velocity vector fields in bifurcation 3-4 for a resting condition: (a) $r/R = 0.4$, (b) $r/R = 0.8$.

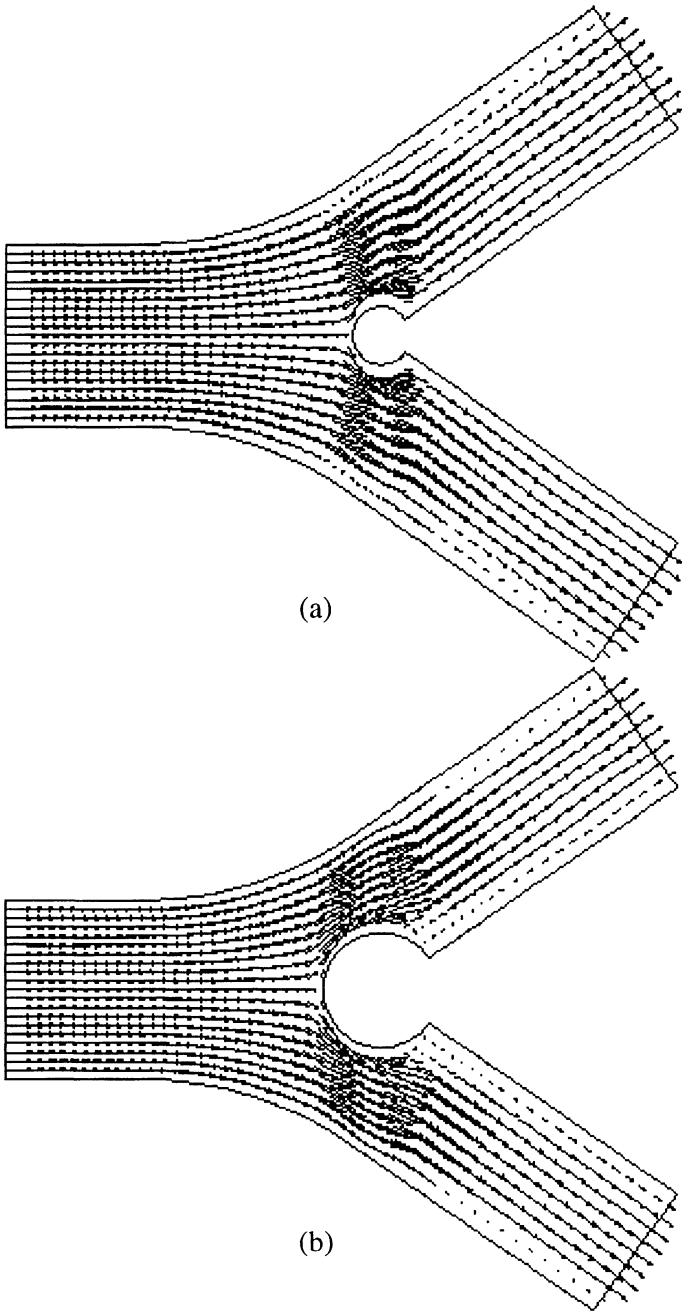


Figure 2: Velocity vector fields in bifurcation 3–4 for exercise: (a) $r/R = 0.4$, (b) $r/R = 0.8$.

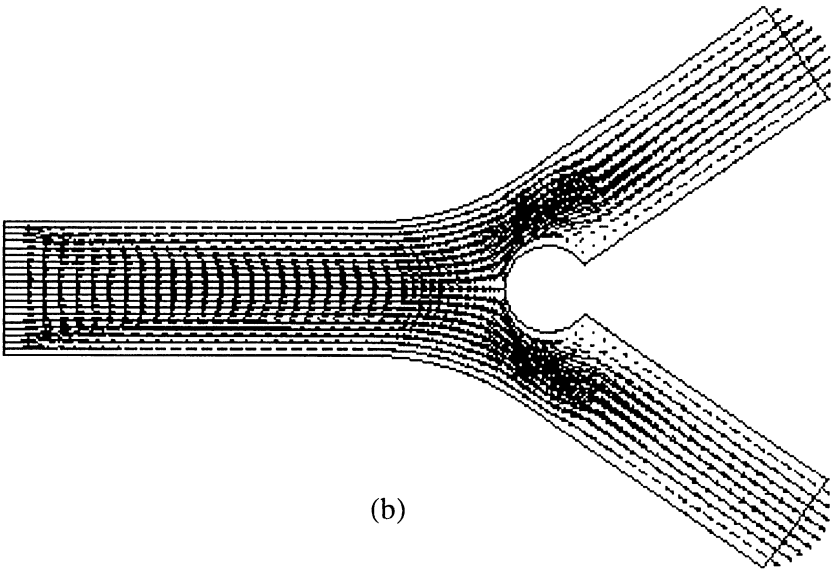
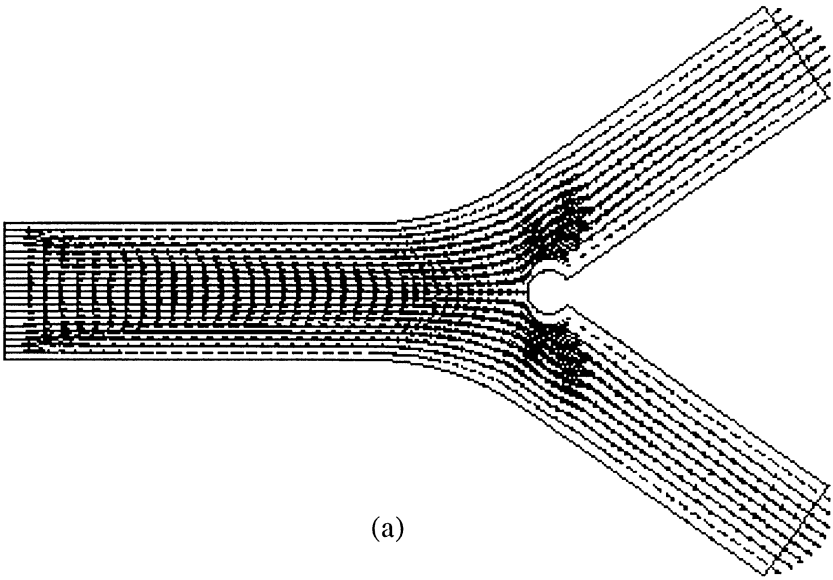


Figure 3: Velocity vector fields in bifurcation 7–8 for a resting condition: (a) $r/R = 0.4$, (b) $r/R = 0.8$.



144 Simulations in Biomedicine IV

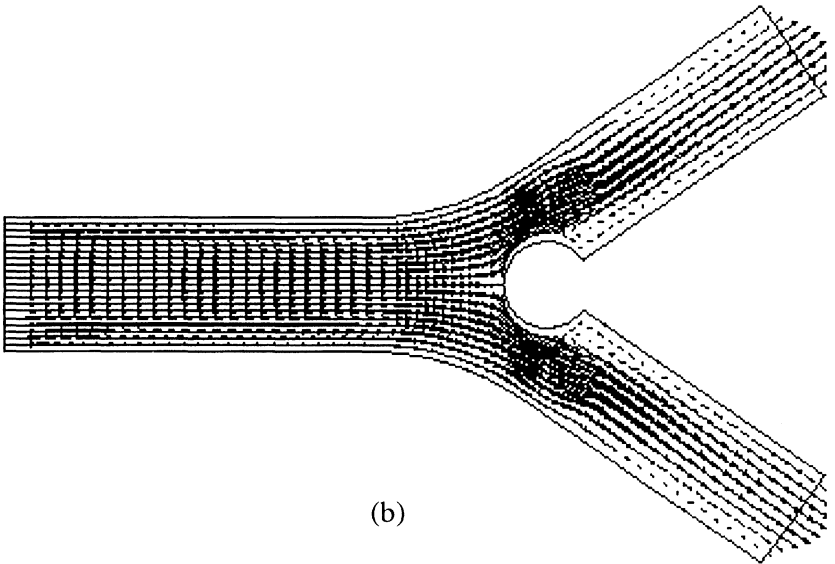
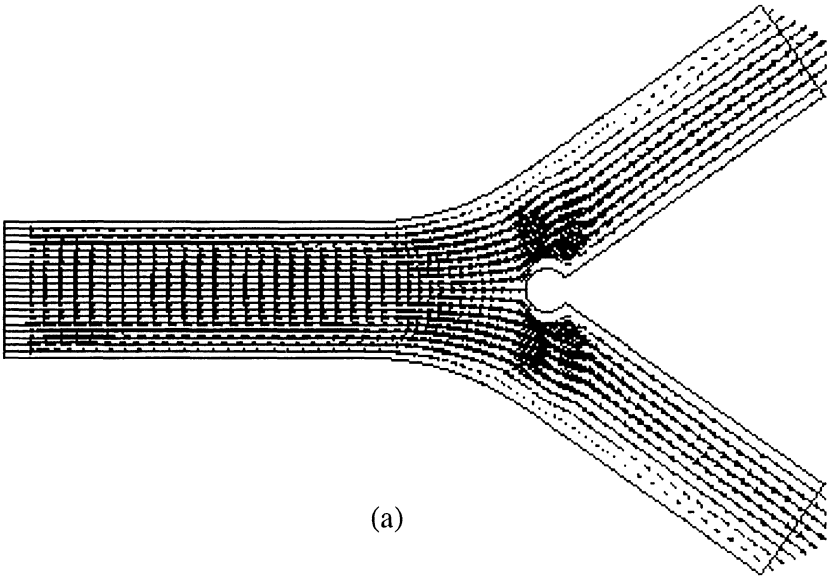


Figure 4: Velocity vector fields in bifurcation 7–8 for exercise: (a) $r/R = 0.4$, (b) $r/R = 0.8$.